Journal of Coastal Research	14	2	660–666	Royal Palm Beach, Florida	Spring 1998

TECHNICAL COMMUNICATIONS

Coastal Surges from Extratropical Storms on the West Coast of the Korean Peninsula

S.-C. Kim†, J. Chen‡, K. Park§, and J.K. Choi††

† Virginia Institute of Marine Science
School of Marine Science
The College of William and Mary
Gloucester Point, VA 23062, USA

‡ National Weather Service
NOAA, W/OSD22
Silver Spring, MD 20910, USA

§ Department of Oceanography
Inha University
Nam-ku, Inchon, Korea

†† Colorado Center for Astrodynamic Research
University of Colorado
Boulder, CO, 80309, USA

ABSTRACT

KIM, S.-C.; CHEN, J.; PARK, K., and CHOI, J.K., 1998. Coastal surges from extratropical storms on the west coast of the Korean Peninsula. *Journal of Coastal Research,* 14(2), 660–666. Royal Palm Beach (Florida), ISSN 0749-0208.

Coastal surges along the west coast of the Korean Peninsula from extratropical storms were investigated using tide gage observations for one year and numerical model hindcasting. Positive surges were associated with smaller scale meteorological forcing than negative surges. Spatial and temporal variations among different locations characterized typical surge propagation from south to north along the west coast and from west to east across the Yellow Sea. Forecasting is feasible with meteorological forcing input with around 1°–1.5° spatial and 6 hourly temporal resolutions.

ADDITIONAL INDEX WORDS: *Extratropical storms, storm surges, coastal hazards, Korean Peninsula, Yellow Sea.*

INTRODUCTION

The water level variability along the west coast of the Korean Peninsula has shown responses associated with meteorological events. The significant portion of subtidal water level fluctuations are considered as storm surges. Storm surge is defined as the oscillation of the water level in a coastal water body resulting from the atmospheric weather system (MURTY, 1984, p. 1) and practically determined by the difference between the observed water level and the predicted astronomical tide. The surge ranges along the Korean west coast are typically below 1 m whereas the Chinese coasts at the opposite side of the Yellow Sea and in the Bohai Bay have experienced significant surge events. Historically, record high surge of 5.2 m at the Korean west coast was reported associated with July 25, 1965 tropical storm event (MURTY, 1984, p. 807). However, there are significant differences between surges associated with tropical and extratropical cyclones. The length and time scales for extratropical storm surges (~100 km and ~ tidal cycle) are much longer than those for tropical storm surges (~10 km and ~ hour). In addition, each extratropical cyclone is associated with different wind and pressure characteristics.

A numerical model is a viable tool for forecasting and hindcasting storm surges. PROCTOR and WOLF (1989), for example, demonstrated the use of numerical models for the storm surge study during a passage of a storm in the North Sea. The U.S. National Weather Service (NWS) has developed a numerical extratropical storm surge forecast model for the US East Coast (KIM *et al.*, 1996; ET model hereafter). This model was also expanded for Norton Sound, Alaska (BLIER *et al.*, 1996). The ET model was initialized with the atmospheric forcing given by the NWS's Aviation (AVN) model (KALNAY *et al.*, 1990). The European Center for Medium-range Weather Forecast model (ECMWF winds hereafter) also provides global surface winds archive which could be alternative or complementary to the AVN model.

In this paper, we will investigate the coastal surges associated with particular extratropical meteorological con-

96070 received 30 June 1996; accepted in revision 2 January 1997.

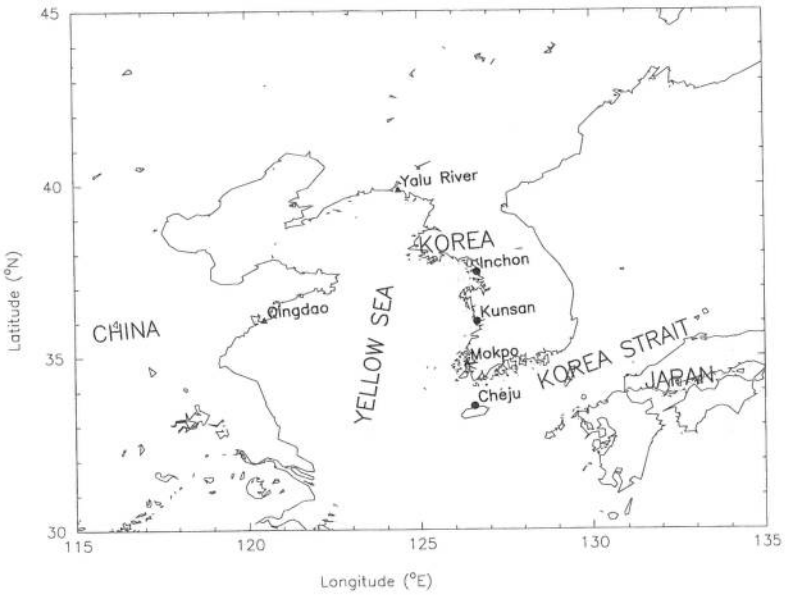

Figure 1. Location map. Filled circles are the tide gage locations used in this study. Filled triangles represent additional locations to investigate coastal surge behavior.

ditions using one-year record from selected tide gages in the Korean west coast and analyzed surface winds. We will simulate coastal surge hindcast by applying the ET model for the Yellow Sea with the ECMWF winds. The simulation combined with the observation will first enable us to characterize the coastal surges from extratropical storms and then provide the feasibility of forecasting the surges.

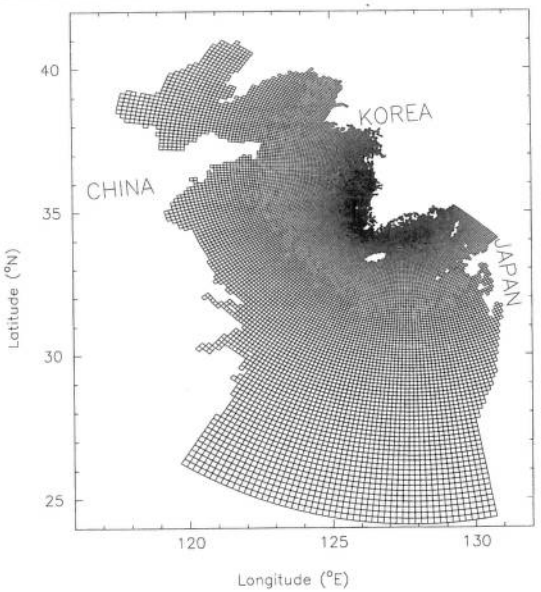

Figure 2. Computational grid. Note the highest resolution (~5 km) is set along the southwestern tip of the Korean Peninsula.

METHODS AND MATERIALS

One year hourly records for 1990 from three selected gages at Inchon, Kunsan, and Cheju along the Korean west coast from north to south (Figure 1) were first low-pass filtered (30 hour period) to represent subtidal frequency. A band-pass filter in the range of 30 hour to 300 hour periods was applied separately to remove seasonal and spring-neap cycle variation in addition to tidal frequencies. An analytical elliptical/ hyperbolic grid (JELESNIANSKI *et al.*, 1992) with 140 by 200 cells (Figure 2) was constructed to cover the entire Yellow Sea as well as the East China Sea and the Korea Strait. The highest spatial resolution (~5 km) is set along the southwestern tip of the Korean Peninsula. At the center of each grid cell, depth was interpolated from nautical charts. The spatial resolution of the ECMWF winds was approximately 1.125° in both latitude and longitude. We applied linear interpolation between 6-hourly projections of the ECMWF winds. The linear interpolation is restricted to the extratropical systems. For shorter time-scaled tropical systems with steep gradients, linear interpolation would result in erroneous representation of transitional stage. Surface pressure data was not used for the simulation in this study because orographic effect was not removed. Using the ET model, we simulated one year hindcast of coastal surges with 120-hour spin-up period and 90-second time step for the ET model.

TIDE GAGE DATA

Figure 3 shows the subtidal signal at Inchon and surface pressure and north-south wind velocity extracted from the ECMWF winds at a location (36.448 °N and 124.875 °E) in the middle of the Yellow Sea. This point was chosen to

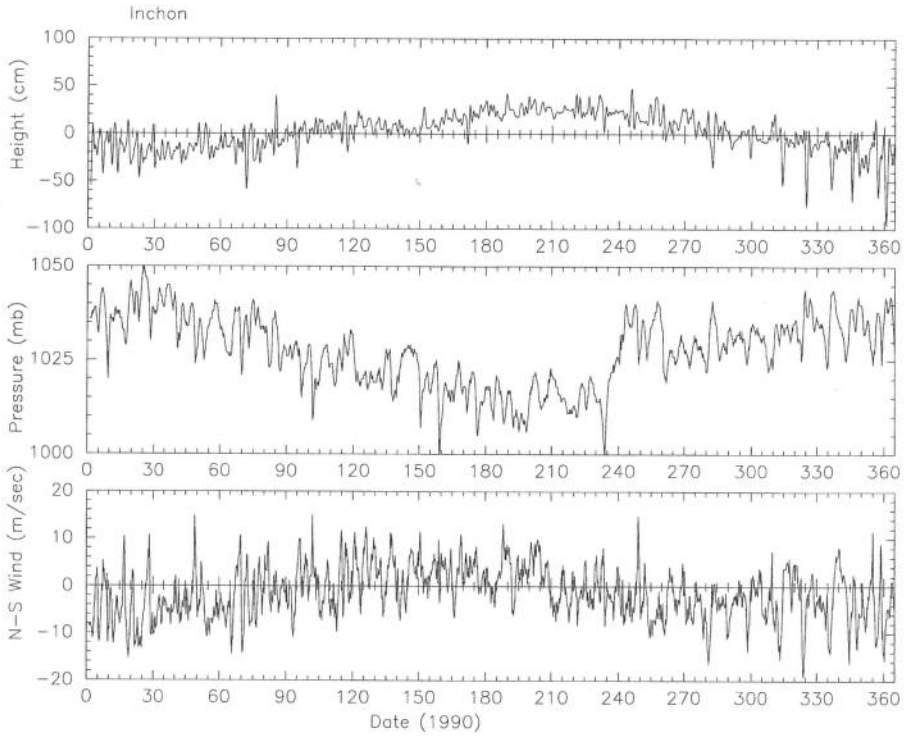

Figure 3. One year subtidal signal from tide gage at Inchon and meteorological conditions of the Yellow Sea (36.448 °N and 124.875 °E). The meteorological conditions were given by sea surface pressure in mb and north–south component of surface wind.

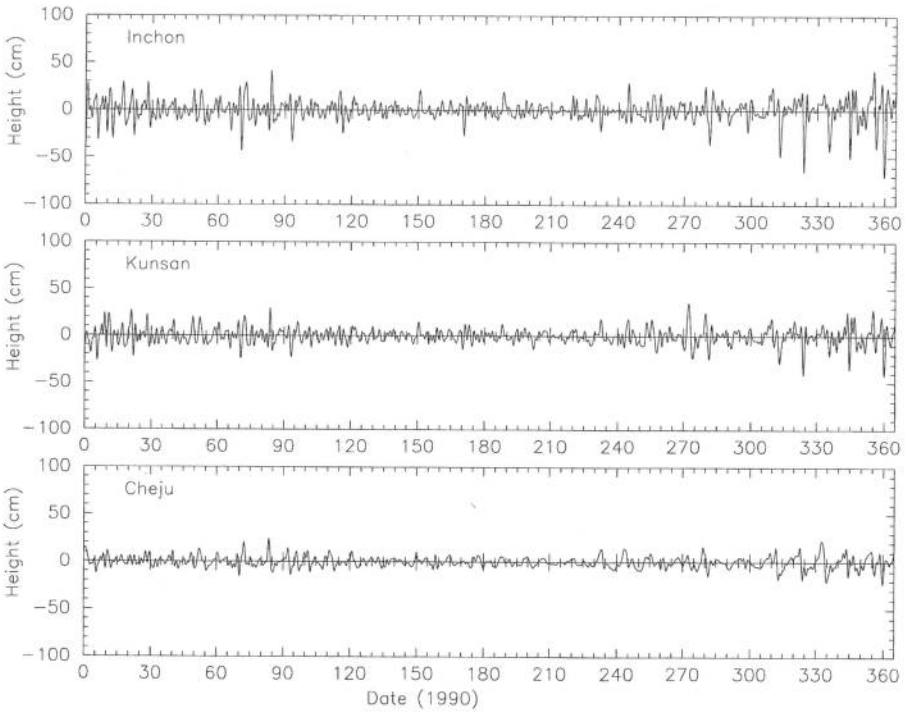

Figure 4. One year surge records from three tide gage locations—Inchon, Kunsan, and Cheju from north to south.

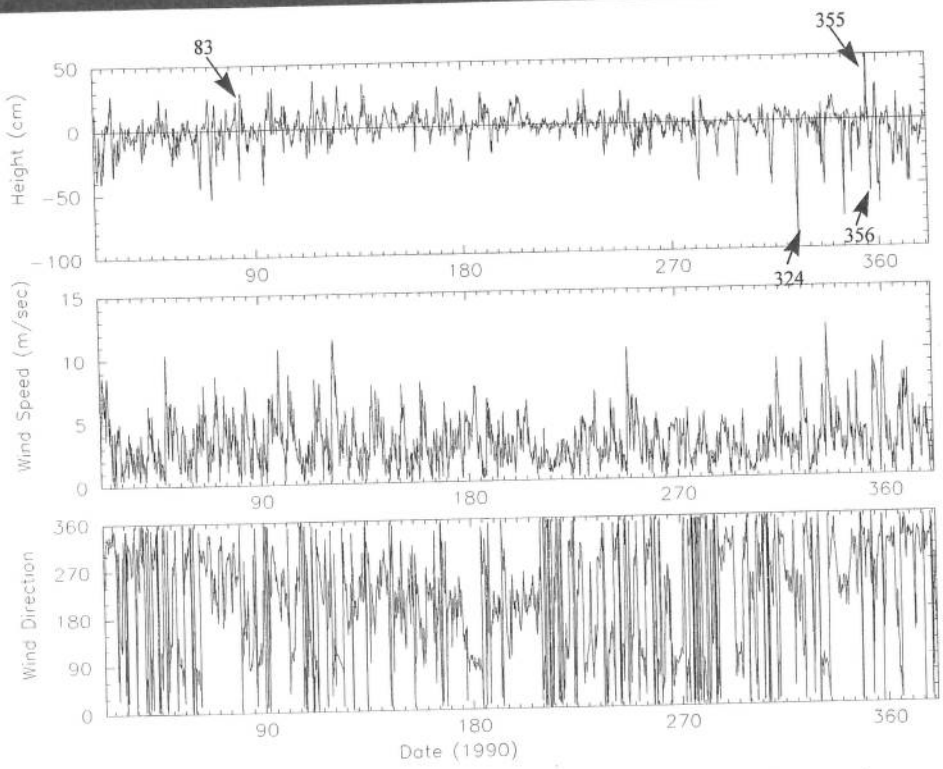

Figure 5. Surges and local winds at Inchon. Note 0° is northerly, 90° is easterly, 180° is southerly, and 270° is westerly.

represent meteorological conditions of the Yellow Sea and considered having minimal orographic effect. The cross-correlation coefficients, ρ, of the subtidal signal at Inchon to the surface pressure and north-south wind at peaks were −0.81 and 0.56, respectively. This points out the meteorological control over sea level. The sea level signal lags meteorological variables by approximately 1 day.

The band-pass filtered data (surge data hereafter) show coherent signal variations among three gages (Figure 4), fitting the scales for extratropical systems (~ order of 100 km). The peak ρ between Inchon and Kunsan and between Inchon and Cheju were 0.87 and 0.63, respectively. Inchon's surge was led at Kunsan and Cheju by about 2 and 4 hours, respectively. The peak ρ between Kunsan and Cheju was 0.67. This indicates that Cheju was influenced by different dynamics of the Korea Strait in addition to the Yellow Sea dynamics. More variations in surge signals during cold season than during warm season are related to extratropical weather patterns. Summer season is subject to smaller scale disturbance of tropical origin thus responding signal could be removed by low-pass filtering.

Surge variations during 1990 were small (less than 1 m) compare to the average 4 m tide range along the Korean west coast. But, considering the nature of well-sheltered environment of gage locations, actual coastal surges would have been amplified. At Inchon, relevant high surge events with over 30 cm height deviation occurred in around March 24 (day 83) and December 21 (day 355), while number of significant negative surge events with over 50 cm height deviation were observed during November and December. These events were associated with surface winds of strong northerly component (~ 15 m/sec) (Figure 3). With conspiring high waves from strong winds, the implication of negative surge is a possible threat to navigation in shallow water and change in morphodynamics by redistributing of nearshore bottom sediments.

The peak around day 245 (September 2) coincides with the Tropical Storm No. 15. Because of different scales of tropical storm events, cautious use of filtered data must be addressed. For a tropical storm surge, relative position of peak surge time becomes critical because peak surge would last only in the order of hours. It is beyond the scope of this study to deal with tropical storm surges.

SURGE HINDCASTS

The ET model is based on depth-integrated shallow water equations. Surface stress and pressure gradient control the surge behavior through bottom stress and Coriolis force. Nonlinear advective terms as well as horizontal viscosity terms are neglected. The ET model also does not account for the steric effects. The hydrostatic effect of sea surface pressure was not included in this study to elude the orographic effect of the ECMWF surface pressure.

A storm surge is primarily a barotropic response of coastal water to atmospheric forcing, with control of coast-

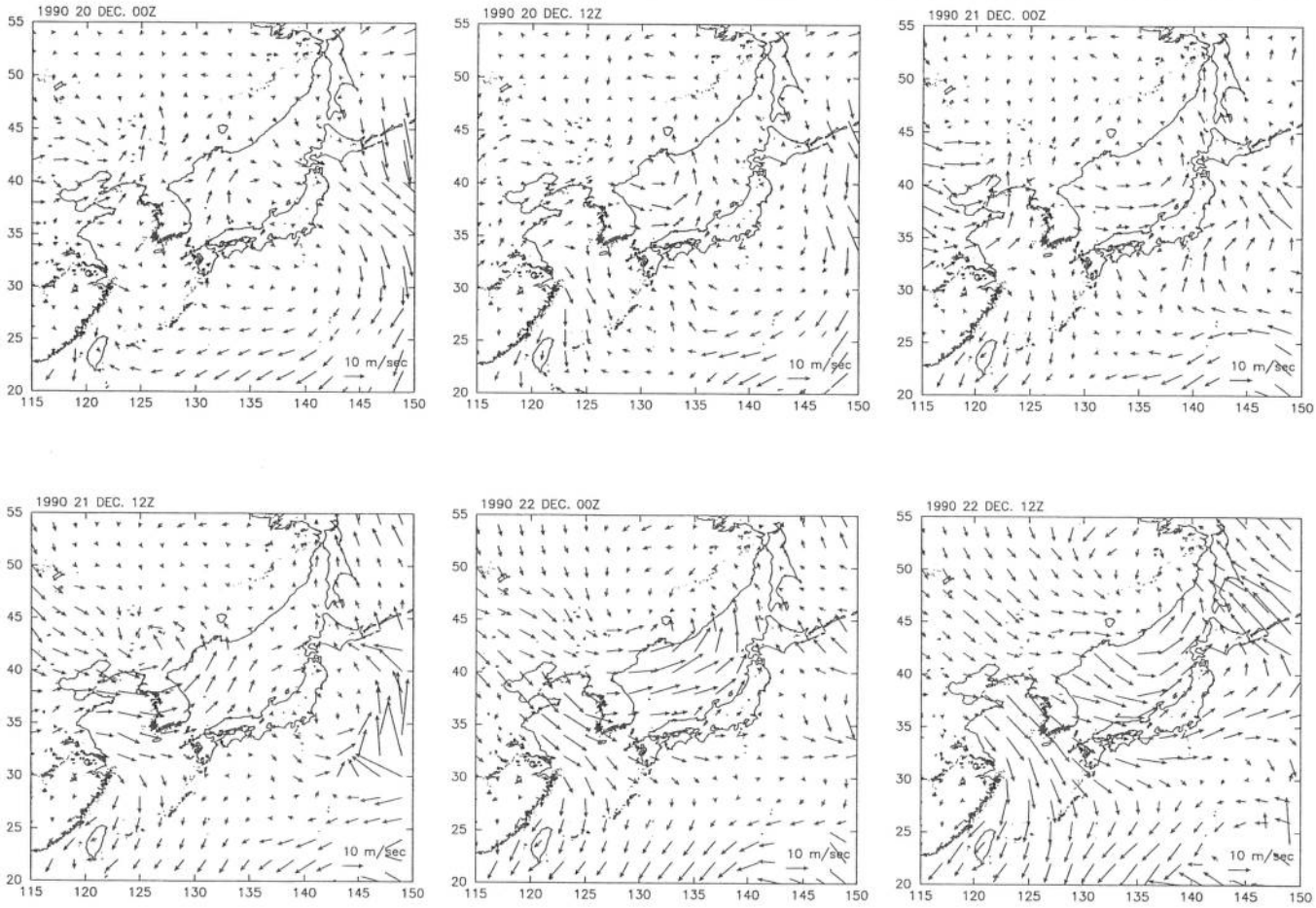

Figure 6. Surface winds during a combined positive and negative surge event around day 355 (December 21).

line geometry and bathymetry of nearshore region. Shallow water interactions amplify surges whereas friction interactions dampen them. The correlation coefficient between simulation and observation is 0.63 at Inchon and reduced to 0.48 at Cheju. The root-mean-square (rms) errors of the simulated surges to observed surges are 0.27 cm at Inchon, 0.23 cm at Kunsan, and 0.15 cm at Cheju, respectively. These are approximately less than 3% of standard deviations. This suggests that the model simulation was successful and the wind input and the model basin geometry to be used with the ET model were adequate.

Figure 5 shows surge variations and local winds at Inchon. It is apparent that the negative surges occur when northerly components (0°–90° and 270°–360°) prevail. Positive surges seem to be associated with southerly (90°–270°) winds but the relationships are not as distinct. Surge event at day 355 (December 21) followed by negative surges at day 356 (December 22) is a typical event associated with cyclone passage (Figure 6). First, southwesterly winds (December 21) pushed water toward the Korean west coast, causing 50 cm surge. Then, shifting winds from southwesterly to northwesterly (December 22) drained the water from the coast, resulting in −50 cm negative surge. Positive surges propagated from south around day 83 (March 24) were due to southeasterly winds associated with anticyclone motion (Figure 7). Later stage shows long fronts extended over the southern portion of the Yellow Sea. Typical negative surge event around day 324 (November 20) was due to persistent northerly winds associated with an anticyclone moving south (Figure 8). Typically, the spatial scale of surface winds responsible for negative surges (Figure 8) was larger than that for positive surge (Figure 7): a negative surge responds to low gradient winds of larger spatial scale whereas a positive surge is related to high spatial gradients.

In order to investigate the spatial variation of storm surges in the Yellow Sea, we calculated ρ for the surges from selected stations with respect to Inchon (Table 1). This exemplifies the surges propagate typically from south (Cheju) to north (Yalu River) and from west (Qingdao) to east (Inchon). The high cross-correlation between Inchon and Kunsan also indicates the length scale of 100 km for extratropical storm surges. Along the Korean west coast,

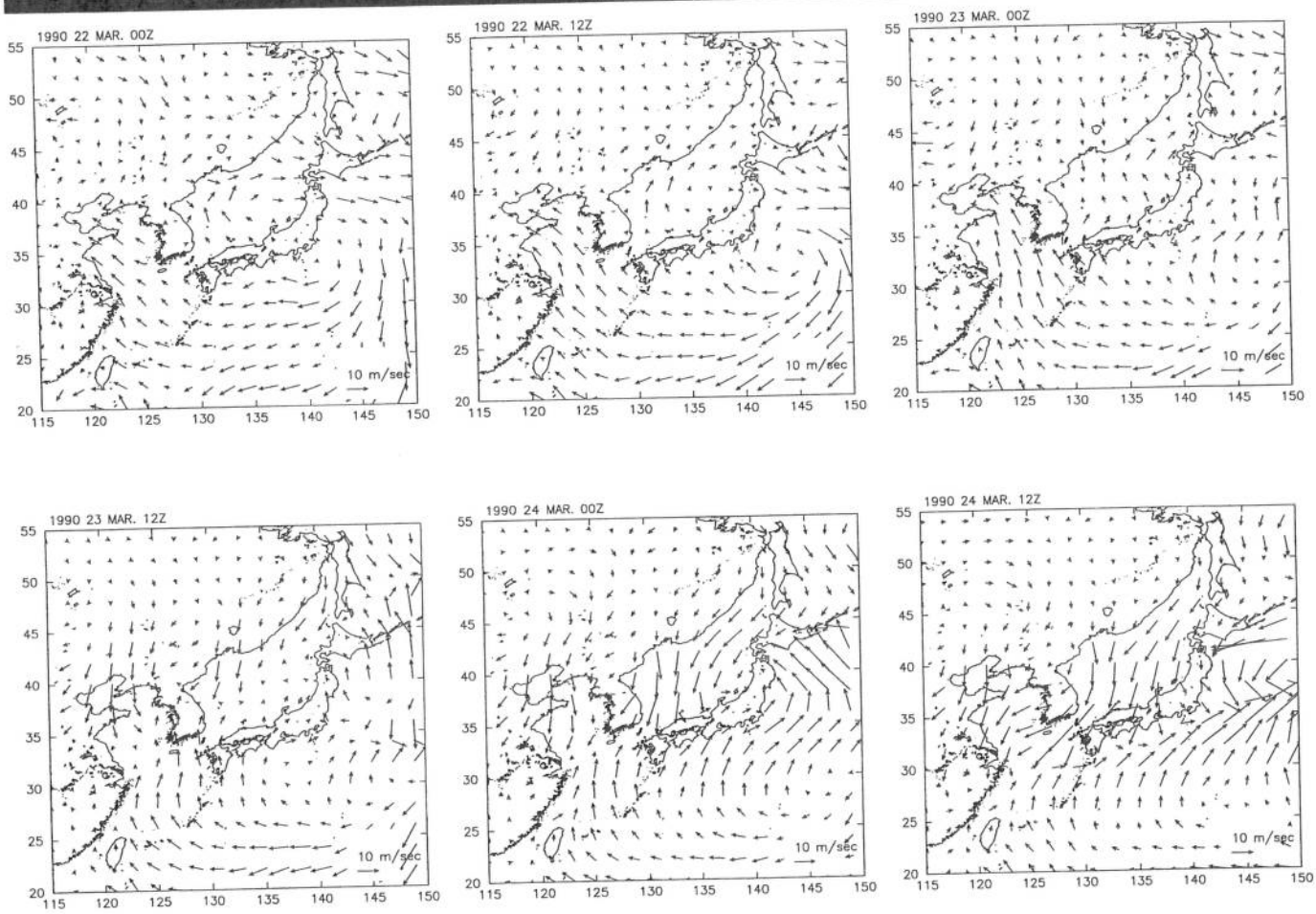

Figure 7. Surface winds during a surge event around day 83 (March 24).

higher variations were observed north of Inchon compared to the southern region, related to the land boundary of the northern Yellow Sea.

CONCLUDING REMARKS

In this study, extratropical storm surge hindcast using the ET model with the ECMWF winds was attempted. The results showed the first order accuracy of the hindcast to the band-pass filtered tide gage data. This implies that it is feasible to forecast the surge forecast with reasonable meteorological input of comparable spatial and temporal spacing of the ECMWF winds (about 1.125° and 6 hourly). We did not test for the static effects of sea surface pressure. However, it appears that surface winds have first order responsibility to coastal water level changes.

Surge characteristics, such as the longer scale that characterizes negative surges and south-north propagation, define the primary response of the Yellow Sea to a meteorological forcing. The significance of coastal surges increases from south to north along the Korean west coast.

The filtering method used in this study is only a temporary substitute for real surge calculations which is determined by subtracting astronomical tidal prediction from observed water level. The ET model does not include tide-surge interactions (*e.g.* WOLF, 1981) which may be pertinent especially in the macrotidal environment such as the Korean west coast. The ET model's capacity of resolving vertical structure of currents, though limited, may be useful for the study of transport related problems such as oil spill and sediment transport. We may need to develop a three-dimensional model in this regard as Heaps (1983) pointed out.

Table 1. *Cross-correlation coefficients among gage stations with respect to Inchon.*

Station	Cross-Correlation Coefficient	Lag (hours)
Qingdao	0.45	12
Yalu River Entrance	0.76	−2
Inchon	1.00	0
Kunsan	0.91	1
Mokpo	0.71	3
Cheju	0.64	6

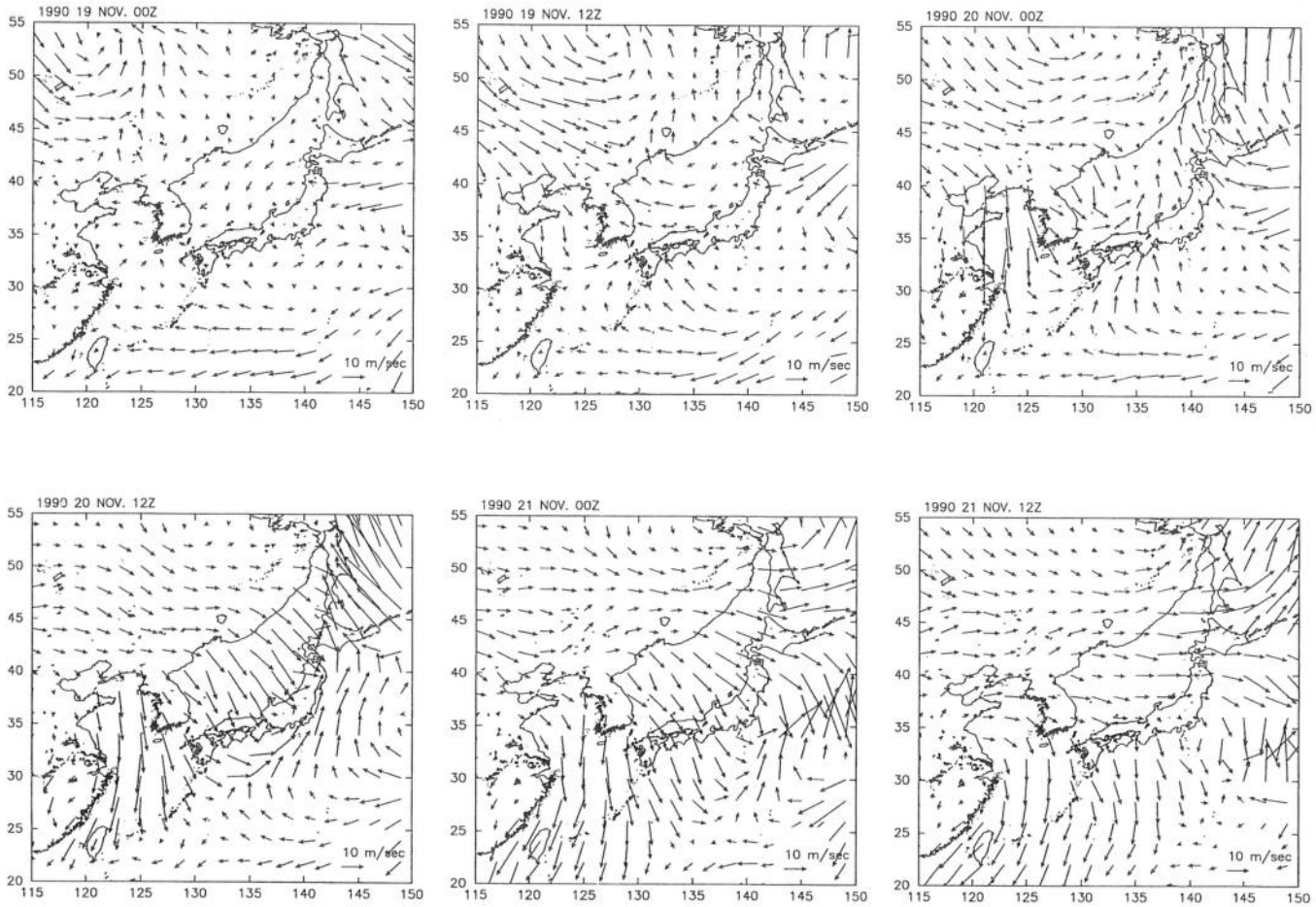

Figure 8. Surface winds during a negative surge event around day 324 (November 20).

ACKNOWLEDGEMENTS

Tide gage data was provided by Prof. Phil-Sung Park of Suwon University, Korea. Dr. Wright of VIMS provided helpful suggestion and manuscript review. This is Contribution number 2059 from the Virginia Institute of Marine Science.

LITERATURE CITED

BLIER, W.; KEEFE, S.; SHAFFER, W.A., and KIM, S.-C., 1996. Observation and numerical modeling investigations of three Bering Sea storms and their associated storm surges in the region of Nome, Alaska. *Proceedings, Conference on Oceanic and Atmospheric Prediction* (Atlanta, Georgia, American Meteorological Society), pp. 272–280.

HEAPS, N.S., 1983, Storm surges, 1967–1982. *Geophysical J. Royal Astronomical Soc.*, 74, 331–376.

JELESNIANSKI, C.P.; CHEN, J., and SHAFFER, W.A., 1992. SLOSH: Sea, lake, and overland surges from hurricanes. *NOAA Technical Report NWS 48*, U.S. Department of Commerce, 71p.

KALNAY, E.; KANAMITSU, M., and BAKER, W.E., 1990. Global numerical weather prediction at the National Meteorological Center. *Bulletin of American Meteorological Society*, 71, 1410–1428.

KIM, S.-C.; CHEN, J., and SHAFFER, W.A., 1996. An operational forecast model for extratropical storm surges along the U.S. East Coast. *Proceedings, Conference on Oceanic and Atmospheric Prediction*, (Atlanta, Georgia, American Meteorological Society), pp. 281–286.

MURTY, T.S., 1984. Storm surges. *Canadian Bulletine of Fisheries and Aquatic Sciences 212*, 897p.

PROCTOR, R. and WOLF, J., 1989. An investigation of the storm surge of February 1, 1983 using numerical model. *In:* DAVIES, A.M., (ed.), *Modeling Marine Systems*. Boca Raton, Florida: CRC Press.

WOLF, J., 1981. Storm-tide interaction in the North Sea and River Thames. *In:* PEREGRINE, D.H., (ed.), *Floods Due to High Winds and Tides*. New York: Academic.